veterinary sciences

MDPI

Article

Rapid and Visual Detection for Raccoon Dog-Associated Canine Coronavirus via Combination of Multienzyme Isothermal Rapid Amplification and Lateral Flow Dipstick

Shaohua Qi [1], Sifan Cao [2] and Xianzhu Xia [3,*]

[1] Institute of Laboratory Animal Sciences, Chinese Academy of Medical Sciences & Peking Union Medical College, Beijing 100020, China; qishaohua0902@163.com
[2] College of Animal Medicine, Northeast Agricultural University, Harbin 150069, China; sifancao@163.com
[3] Changchun Veterinary Research Institute, Chinese Academy of Agricultural Sciences, Changchun 130000(130022), China
* Correspondence: xiaxzh@cae.cn

Simple Summary

A multienzyme isothermal rapid amplification combined with a lateral flow dipstick assay targeting the nucleocapsid gene of canine coronavirus and the raccoon dog-associated lineage was developed. The assay detected standard plasmid DNA at concentrations as low as 10^1 copies per microliter within 20 min. It is simple, rapid, sensitive, specific, and reproducible, making it suitable for on-site testing.

Abstract

Canine coronavirus (CCoV) is a major enteric pathogen that infects both dogs and raccoon dogs. The raccoon dog-associated canine coronavirus causes epizootic catarrhal enteritis and significant economic losses in the fur industry. In this study, a diagnostic test was developed by integrating multienzyme isothermal rapid amplification (MIRA) with lateral flow dipstick (LFD) technology, targeting the highly conserved nucleocapsid protein gene of CCoV. The assay demonstrated the capability to detect as low as 10^1 copies/μL of standard recombinant plasmids within a 20-min timeframe at 35 °C. Notably, the assay successfully detected both the raccoon dog-associated canine coronavirus and a canine CCoV strain, demonstrating its cross-host detection capability. Furthermore, a preliminary evaluation of 30 clinical samples was conducted using both the RT-qPCR method and the newly developed MIRA-LFD method, yielding a 100% overall agreement (positive percent agreement: 100%, 95% CI: 84.6–100%; negative percent agreement: 100%, 95% CI: 63.1–100%). The MIRA-LFD assay also exhibited high specificity, showing no cross-reactivity against other tested viral nucleic acids, confirming its potential as a rapid diagnostic tool for CCoV screening.

Keywords: multienzyme isothermal rapid amplification; lateral flow dipstick; raccoon dog-associated canine coronavirus; rapid nucleic acid detection

Check for updates

Academic Editor: Shuanghui Yin

Received: 21 October 2026
Revised: 26 November 2026
Accepted: 27 November 2026
Published: 29 November 2026

Copyright: © 2026 by the authors. Licensee MDPI, Basel, Switzerland. This article is an open access article distributed under the terms and conditions of the Creative Commons Attribution (CC BY) license.

1. Introduction

The raccoon dog-associated canine coronavirus (CCoV) is an enveloped, single-stranded positive-sense RNA virus belonging to the *Alphacoronavirus-1* species [1]. Recent studies have demonstrated that CCoV strains from diarrheic raccoon dogs form a distinct lineage [2]. Although not a distinct species, based on traditional epidemiological naming conventions related to the host of origin, we refer to this specific raccoon dog-associated

CCoV lineage as RDCoV throughout this study. Infection usually causes mild to moderate gastrointestinal signs, such as diarrhea and vomiting, but can be associated with substantial mortality [3]. Although vaccines exist for dogs, their efficacy in preventing viral shedding is debated, and no specific therapeutics are available for this virus, leading to significant economic losses in the breeding industry. Consequently, there is an urgent necessity to develop a rapid, simple, and on-site detection method for CCoV (including the RDCoV lineage) to support disease prevention and timely control measures.

At present, RT-qPCR and conventional PCR are widely used for the clinical identification of viral pathogens; however, these thermal cycling-based methods require sophisticated and expensive equipment, as well as trained personnel, which severely limits their application for rapid, on-site detection in resource-limited farm settings [4,5]. To overcome these limitations, there is an urgent need for a rapid, simple, and minimally equipped diagnostic tool.

Isothermal amplification techniques, particularly multienzyme isothermal rapid amplification (MIRA), offer a promising alternative. MIRA utilizes a novel recombinase, helicase gp41, and recombinase recA from Streptomyces coelicolor to invade double-stranded DNA, distinguishing it from RPA and RAA. (the detailed reaction mechanism is illustrated in Supplementary Figure S1). This technique provides stable and rapid amplification at a constant temperature, eliminating the need for complex thermal cyclers. Furthermore, MIRA is comparatively more cost-effective than RT-PCR, making it highly suitable for large-scale on-site rapid detection.

Therefore, we developed a MIRA-LFD assay for the visual detection of CCoV (including the raccoon dog-associated lineage). This approach addresses the urgent need for rapid, simple, and minimally equipped diagnostics, offering a promising tool for on-site screening in resource-limited veterinary clinics and farms.

2. Materials and Methods

2.1. Virus Strains and Fecal Swabs

The raccoon dog-associated canine coronavirus strain RDCoV/CL/2022 (OR082962) and other fecal swabs of raccoon dogs used in this study were obtained from the Special Animal and Plant Institute of the Chinese Academy of Agricultural Sciences (CAAS) fur animal breeding farm in Zuoji Town, Changyi District, Jilin City, Jilin Province, China, in 2022. The RDCoV/CL/2022 viral RNA was used for plasmid construction. All samples were collected non-invasively during routine clinical veterinary diagnostics. No animal experiments were performed in this study, and therefore, specific ethical approval was not required.

2.2. RNA Extraction and cDNA Synthesis for Plasmid Construction

Viral RNA was extracted from RDCoV/CL/2022 using the RNA Extraction Kit (Tiangen Bio-Tech, Beijing, China)and reverse-transcribed into cDNA with the HiScript III 1st Strand cDNA Synthesis Kit (+gDNA wiper) (Vazyme Biotech, Nanjing, China) for the subsequent cloning of the *N* gene. Samples were stored at −80 °C.

2.3. Cloning of Standard Recombinant Plasmids

The nucleoprotein gene of RDCoV/CL/2022 was identified as an optimal target gene for MIRA-LFD. The cDNA was amplified with N-specific forward and reverse primers and cloned into pMD-20T vector (Takara Biomedical Technology Co., Ltd., Beijing, China) to construct pMD-20T-N plasmid. The primers used for conventional PCR were designed in this study, and their sequences are listed in Table 1. The plasmid was sequenced by Sangon Biotech (Shanghai, China) and quantified with a NanoDrop One spectrophotometer

(NanoDrop™ One, Thermo Fisher Scientific, Waltham, MA, USA). The insert length of the *N* gene is 1460 bp, the pMD-20T vector length is 2736 bp, and the total length of the recombinant pMD-20T-N plasmid is 4196 bp. Copy number was calculated as 10^9 copies/μL using the equation below. The template was then serially diluted 10-fold. Nucleic acid samples were stored at −20 °C.

$$\text{DNA copy number}\left(\frac{\text{copies}}{\mu\text{L}}\right) = \frac{\text{DNA concentration}\left(\frac{\text{ng}}{\mu\text{L}}\right) \times 10^{-9}}{\text{DNA length} \times 660} \times 6.02 \times 10^{23}$$

Table 1. The nucleic acid sequence of primers and probes in this study.

Assay	Primers/Probes	Sequence (5′–3′)	Location [1]
Basic MIRA	F1	GGAATAGGTAATAGGGACCAGCAAATTGGTTA	27,149–27,180
	F2	GGACTTATGTCCGAGAGACCTTGTACCCAA	27,118–27,147
	F3	AGGAATAGGTAATAGGGACCAGCAAATTGGT	27,148–27,178
	R1	TTGAGGTCAGCATGAGGTCCTGTTCCTAAGTA	27,254–27,285
	R2	GAGGTCAGCATGAGGTCCTGTTCCTAAGTAA	27,253–27,283
	R3	GAATTATCCCTAGAGTGGTTTGATTCAAGTTG	27,422–27,453
	R4	GGTCAGCATGAGGTCCTGTTCCTAAGTAAT	27,252–27,281
	R5	AGCATGAGGTCCTGTTCCTAAGTAATAGAAAAA	27,245–27,277
MIRA-LFD	F2	GGACTTATGTCCGAGAGACCTTGTACCCAA	27,118–27,147
	R4	Biotin-GGTCAGCATGAGGTCCTGTTCCTAAGTAAT	27,252–27,281
	Pm [2]	6′FAM-CAACTCCGCTATCGCATGGTGAAGGGACAGCGTAA[THF]GATCTACCTGAGAGAT-C3Spacer	27,191–27,242
RT-qPCR	Fq	TGGAAGAGAACTGCAGGTAAAG	27,683–27,704
	Rq	TCAGCCAGTTGTGGGTAATG	27,791–27,810
	Pq [3]	6′FAM-ATGGCGCTAGAAGTAGTTCAGCCAATT-BHQ1	27,723–27,749
PCR	Fp	GCAGGACCATCATCTACACA	26,808–26,827
	Rp	TGGATCAGTCACACCTAAAAC	28,248–28,268

[1] The location refers to the complete genome of the raccoon dog coronavirus strain RDCoV/CL/2022 (GenBank accession no. OR082962). [2] 6′FAM: 6-carboxyfluorescein; THF: Tetrahydrofuran; C3Spacer: C3 spacer at the 3′ end to block elongation. [3] 6′FAM: 6-carboxyfluorescein; BHQ1: Black Hole Quencher 1.

2.4. MIRA Primers and Probe Design

A highly conserved region of the CCoV nucleoprotein gene was selected for primer and probe design. To verify its conservation, a multiple sequence alignment was performed across various CCoV strains, including the target reference strain RDCoV/CL/2022 (GenBank: OR082962) and other raccoon dog-associated strains: RDCoV/CY/34/2022 (OR960568.1), RDCoV/DLZH/2023 (OR965710.1), RDCoV/CY/11/2023 (OR960569.1), RDCoV/CL/64/2023 (OR960570.1), and strain HBCL (MN719179.1). The alignment also included canine CCoV strains: CCoV_191133SY (OQ540914.1), CCoV_191140SY (OQ540915.1), CCoV_191106SY (OQ540912.1), CCoV_191118SY (OQ540913.1), HeB-G1 (OM451123.1), and SD-F3 (OM451122.1). The target sequence was further analyzed using Primer Premier 5.0 software, and three forward primers, five reverse primers, and one probe were designed as detailed in Table 1. For product detection using the lateral flow

dipstick, the reverse primer was 5′-biotinylated. The probe was 5′-FAM-labeled, contained a THF residue replacing a nucleotide near the 3′ end, and had a 3′ C3 spacer [6]. All primers and probes were synthesized by Sangon Biotech (Shanghai, China) and purified by high-performance liquid chromatography (HPLC).

2.5. MIRA Primers Screening MIRA Primer Design and Screening

Fifteen primer combinations were screened using the Basic MIRA Kit (Cat. No.: WLB8201KIT, Amp-Future Biotech Co., Ltd., Weifang, China). The pMD-20T-N plasmid was used as the template at a moderate concentration of 10^3 copies/μL. This concentration was chosen because extremely low or high template concentrations result in insufficient or saturated band brightness, respectively, making it difficult to visually compare amplification efficiency. Each 50-μL reaction contained 29.4 μL of A buffer, 9.1 μL of double-distilled water, 2 μL of forward primer (10 μM), 2 μL of reverse primer (10 μM), 5 μL of plasmid template, and 2.5 μL of B buffer (280 mM). Reactions were incubated in a water bath at 35 °C for 15 min (based on the manufacturer's initial recommendation). MIRA products were purified by phenol–chloroform extraction and analyzed by 2% agarose gel electrophoresis. The optimal primer set was selected based on band brightness and size, the absence of nonspecific amplification, and the absence of primer dimers.

2.6. Optimization of Reaction Temperature and Time for MIRA-LFD Assay

Temperature gradients (15 to 50 °C) were tested using a fixed reaction time of 15 min based on the manufacturer's protocol. Subsequently, time gradients (0 to 14 min) were tested at the optimized temperature of 35 °C. Each experiment was performed independently in triplicate.

2.7. MIRA-LFD Assay

MIRA-LFD was performed with the optimal primer set and probe. Following the manufacturer's instructions for the RNA Isothermal Rapid Amplification Kit (Colloidal Gold Strip Type)-II (Cat. No.: WLRN8209KIT, Amp-Future Biotech Co., Ltd., Weifang, China), each 50 μL reaction contained 29.4 μL of A buffer (which includes the reverse transcriptase and MIRA enzymes), 8.5 μL of double-distilled water, 2 μL of forward primer (10 μM), 2 μL of reverse primer (10 μM), 0.6 μL of Nfo probe (10 μM), 5 μL of viral RNA template, and 2.5 μL of B buffer (280 mM). Viral RNA was directly added as the template, and the reaction was incubated at optimal reaction and time (35 °C, 10 min). Reverse transcription and amplification occurred simultaneously in a single tube. A 10-μL aliquot of the reaction was diluted with 190 μL of double-distilled water. A 50-μL portion of the diluted product was loaded onto the sample pad of a lateral flow dipstick (Amp-Future Biotech Co., Ltd., Weifang, China). Results were read within 5 min.

2.8. Sensitivity Analysis of MIRA-LFD

Ten-fold serial dilutions of the pMD-20T-N plasmid were prepared. For the MIRA-LFD assays, the plasmid was diluted from 10^5 to 10^0 copies/μL. For the conventional PCR and RT-qPCR assays, a broader dilution series from 10^7 to 10^0 copies/μL was used to determine its detection limit. MIRA-LFD reactions were performed at 35 °C for 10 min in a water bath, and products were detected with lateral flow dipsticks. Each experiment was performed independently in triplicate.

RT-qPCR was performed on a C1000 Touch Thermal Cycler (Bio-Rad Laboratories, Inc., Hercules, CA, USA) with the One Step PrimeScript™ RT-PCR Kit (Takara Biomedical Technology Co., Ltd., Beijing, China), Each 20 μL reaction mixture contained 10 μL of 2× One Step RT-PCR Buffer III, 0.4 μL of TaKaRa Ex Taq HS (5 U/μL), 0.4 μL of PrimeScript RT

Enzyme Mix II, 0.4 µL of forward primer (10 µM), 0.4 µL of reverse primer (10 µM), 0.8 µL of probe (10 µM), 2 µL pMD-20T-N template, and 5.6 µL of RNase-free dH2O. Thermal cycling was 95 °C for 5 s, followed by 40 cycles of 95 °C for 3 s and 60 °C for 20 s. Primers and probes are designed in this study (listed in Table 1). PCR was performed on a TGreat Expert PCR amplifier (TIANGEN Biotech Co., Ltd., Beijing, China). The reaction contained Phanta Flash Master Mix, primers, double-distilled water, and pMD-20T-N template. Thermal cycling was 95 °C for 3 min; 35 cycles of 95 °C for 15 s, 55 °C for 15 s, and 72 °C for 85 s; and a final extension at 72 °C for 5 min. Products were analyzed by 2% agarose gel electrophoresis. Primer and probe sequences are listed in Table 1.

2.9. Specificity Analysis of MIRA-LFD

The specificity of the MIRA-LFD assay was evaluated using nucleic acids from eleven viruses: the target raccoon dog-associated canine coronavirus strain (RDCoV/CL/2022), canine coronavirus (CCoV), coronavirus HKU-1, coronavirus OC43, coronavirus NL63, coronavirus 229E, bovine coronavirus, SARS-CoV-2, mink coronavirus, canine distemper virus (CDV), and canine parvovirus (CPV). The pMD-20T-N plasmid was used as the positive control.

Specifically, the nucleic acids of the CCoV, bovine coronavirus, mink coronavirus, CDV, and CPV were provided by the Laboratory of Animal Virology, Changchun Institute of Veterinary Medicine, Chinese Academy of Agricultural Sciences. The human coronaviruses (HKU-1, OC43, NL63, and 229E) were obtained from the NATtrol™ sp RP Multimarker controls kit (Cat. No.: MDZ001, ZeptoMetrix, Buffalo, NY, USA). The SARS-CoV-2 nucleic acid was sourced from the NATtrol™ SARS-CoV-2 (recombinant) Stock (Cat. No.: 0831042, ZeptoMetrix, Buffalo, NY, USA). Reactions were performed under optimized conditions, and products were detected with lateral flow dipsticks.

2.10. Clinical Sample Detection and Statistical Analysis Clinical Sample Collection and Statistical Methods

A total of 30 independent fecal swab samples were collected from a single farm in Jilin Province, China, on 29 November 2022. Viral RNA was extracted from all samples using the Rapid Virus RNA Extraction Kit (HaiGene Co., Ltd., Harbin, China). The extracted RNA was used as the template for the MIRA-LFD assay (as described in Section 2.7). The same RNA samples were also tested by RT-qPCR. Primer and probe sequences for RT-qPCR are listed in Table 1. RT-qPCR was performed on a C1000 Touch Thermal Cycler (Bio-Rad Laboratories, Inc., Hercules, CA, USA) with the following conditions: reverse transcription at 42 °C for 5 min and 95 °C for 10 s, denaturation at 95 °C for 5 s and annealing/extension at 60 °C for 20 s for 40 cycles. Each 20 µL reaction mixture contained 10 µL of 2× One Step RT-PCR Buffer III, 0.4 µL of TaKaRa Ex Taq HS (5 U/µL), 0.4 µL of PrimeScript RT Enzyme Mix II, 0.4 µL of forward primer (10 µM), 0.4 µL of reverse primer (10 µM), 0.8 µL of probe (10 µM), 2 µL of template RNA, and 5.6 µL of RNase-free dH_2O. pMD-20T-N plasmid was used as the positive control, and double-distilled water was used as the negative control. Based on the standard curve equation $y = -3.3506x + 38.139$ (Supplementary Figure S2), the theoretical Cq value at zero concentration (y-intercept) is 38.14. Therefore, samples with a Ct value < 38 were considered positive, while those with a Ct value ≥ 38 or no amplification were considered negative. Results from MIRA-LFD and RT-qPCR were compared by Cohen's kappa and McNemar's test. The 95% confidence intervals (CIs) for positive percent agreement (PPA), negative percent agreement (NPA), and overall agreement were calculated using the Clopper–Pearson exact method. A p-value < 0.05 was considered statistically significant. All statistical analyses were performed using R software (version 4.2.1; R Foundation for Statistical Computing). The Clopper–Pearson 95%

confidence intervals for PPA, NPA, and OPA were calculated using the binom.test() function. Cohen's kappa with 95% CI was calculated using the kappam.flexible() function from the irr package with 1000 bootstrap resamples. The exact McNemar's test was performed using the mcnemar.exact() function from the exact2x2 package.

3. Results

3.1. MIRA Primers ScreeningScreening of MIRA Primer Combinations

Gel electrophoresis (Figure 1) showed that the bands corresponding to F2R1 (168 bp), F2R2 (166 bp), F2R3 (336 bp), and F2R4 (164 bp) produced brighter bands than the other combinations, with no nonspecific bands or primer dimers. According to the principle of MIRA primer design, longer MIRA amplicons can reduce detection sensitivity. Consequently, F2R4, which produced the shortest amplicon, was selected as the MIRA primer set. The location of primer group F2R4 and probe Pm is shown in Supplementary Figure S3.

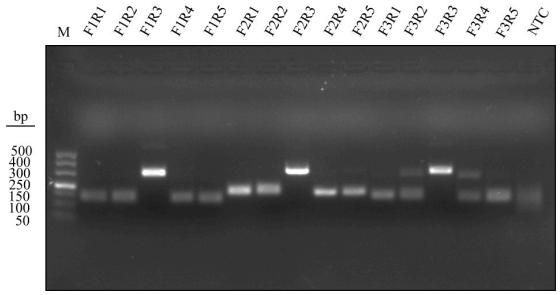


Figure 1. CCoV MIRA primer group screening. The primer name is shown above each lane. The assays were performed at 35 °C for 15 min. The expected product sizes are indicated on the right side of the gel image (F2R1: 168 bp, F2R2: 166 bp, F2R3: 336 bp, and F2R4: 164 bp). The reaction products were detected by 2% (*W*/*V*) agarose gel electrophoresis (AGE). The amplification template is pMD-20T-N plasmid. Lane 17 displayed the negative control (NTC). M: DL2000 DNA Marker.

3.2. Optimization of Temperature and Time for MIRA-LFD Assay

The outcomes of amplification conducted under various temperature gradients were evaluated utilizing dipsticks, as depicted in Figure 2a. The MIRA-LFD demonstrated reactivity within a temperature range of 20 °C to 45 °C. Notably, the color intensity observed on the testing line of the strip reached its maximum at temperatures up to 35 °C, indicating that the optimal temperature for the reaction is 35 °C.

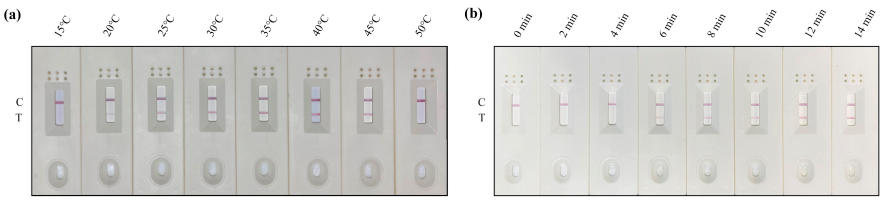


Figure 2. Optimization of reaction temperature and time for CCoV MIRA-LFD assay. (**a**) Optimal reaction temperature of the MIRA–LFD assay. The figure shows the LFD results of MIRA amplification at 15, 20, 25, 30, 35, 40, 45, and 50 °C for 15 min. The temperature is displayed at the top of each dipstick. The amplification template is pMD-20T-N plasmid. C: control line. T: testing line. (**b**) Optimal reaction time of the MIRA–LFD assay. The image shows the LFD results of MIRA amplification at 35 °C for 0, 2, 4, 6, 8, 10, 12 and 14 min. The time to perform the MIRA reaction is displayed at the top of each dipstick. The amplification template is pMD-20T-N plasmid. C: control line. T: testing line.

The products of different reaction times were also detected by the dipstick. The observations indicated that the testing line on the dipstick underwent a color transformation to red in 6 min, intensifying gradually until the 10 min interval (Figure 2b). Subsequently, the color intensity of the line stabilized, indicating that the optimal reaction time for this procedure was established as 10 min.

3.3. Sensitivity Analysis of MIRA-LFD Assay

The analytical limit of detection (LOD) of MIRA-LFD was evaluated using 10-fold serial dilutions of the pMD20T-N plasmid ranging from 10^5 to 10^0 copies/μL. The analytical LOD was determined to be 10^1 copies/μL. For comparison, conventional PCR was tested with a dilution series from 10^7 to 10^0 copies/μL, and its LOD was 10^3 copies/μL. RT-qPCR was tested with the same series as conventional PCR (10^7 to 10^0 copies/μL) and detected down to 10^1 copies/μL (Figure 3). Thus, MIRA-LFD was 100-fold more sensitive than conventional PCR and comparable to RT-qPCR.

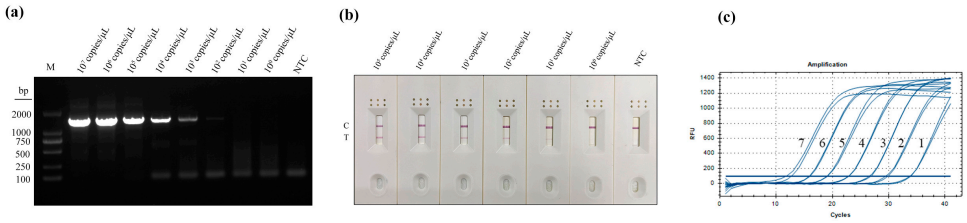


Figure 3. The sensitivity comparison of CCoV MIRA-LFD, PCR, and RT-qPCR assays. (**a**) The sensitivity of PCR assay. The concentrations of each plasmid are indicated on the top of lanes. Lane 10 displayed the negative control (NTC). M: DL2000 DNA Marker. (**b**) The sensitivity of MIRA-LFD assay. The concentrations of each plasmid are indicated on the tops of dipsticks. NTC: negative control. C: control line. T: testing line. (**c**) The sensitivity of the RT-qPCR assay. The amplification curves correspond to 10-fold serial dilutions of the plasmid standard. The numbers 1 to 7 on the figure represent the standard concentrations ranging from 10^7 to 10^1 copies/μL, respectively.

3.4. Specificity Analysis of MIRA-LFD Assay

The results showed that both the pMD20T-N plasmid and the canine CCoV strain tested positive, while all other viral nucleic acid samples were negative (Figure 4). This indicates that the MIRA-LFD assay exhibits high specificity and can effectively detect both the raccoon dog-associated lineage and the canine CCoV strain, demonstrating its cross-lineage detection capability.



Figure 4. The specificity of CCoV MIRA-LFD assay. The names of each viral nucleic acid are listed at the top of dipsticks. NTC: negative control. C: control line. T: testing line.

3.5. Clinical Sample Detection and Statistical Analysis Clinical Evaluation of the MIRA-LFD Assay

Both methods identified 22 positive and 8 negative samples, yielding a 100% overall agreement. The positive percent agreement (PPA) was 100% (95% CI: 84.6–100%), and the negative percent agreement (NPA) was 100% (95% CI: 63.1–100%). The Cohen's kappa value was 1.000 (95% CI: 0.882–1.000). The results of the clinical sample detection and statistical analysis are shown in Table 2. The raw RT-qPCR amplification curves and the corresponding MIRA-LFD visual readouts for the 30 samples are provided in Supplementary Figure S4. The detailed specimen-level information (including farm origin, clinical status, RT-qPCR Ct values, and MIRA-LFD results) is provided in Supplementary Table S1.

Table 2. Results of clinical sample detection and statistical analysis.

Method	RT-qPCR Positive	RT-qPCR Negative	Total	Agreement (95% CI)
MIRA-LFD Positive	22	0	22	PPA: 100% (84.6–100%)
MIRA-LFD Negative	0	8	8	NPA: 100% (63.1–100%)
Total	22	8	30	Overall: 100% (88.4–100%)

4. Discussion

Raccoon dog-associated canine coronavirus (RDCoV) infection causes acute gastroenteritis. Clinical signs include diarrhea, anorexia, depression, weight loss, and tonic spasms, which contribute to a high recurrence rate and increased mortality, especially in cases of co-infection with canine parvovirus or other enteric viruses [7,8]. Typically, severely affected raccoon dogs often die from diarrhea-induced electrolyte imbalance. In non-fatal cases, the condition negatively impacts the quality of fur, resulting in dryness and sparsity, causing economic losses to the fur industry.

Currently, the predominant methods for coronavirus detection are PCR and RT-qPCR [9], both of which necessitate laboratory settings and additional time for result processing. Furthermore, the stationary nature of laboratory equipment precludes real-time, on-site sample analysis, thereby limiting the potential for rapid initial detection. To overcome these limitations, isothermal amplification methods have gained attention. MIRA, a modified version of RPA and RAA, offers several practical advantages [10–15]. So far, MIRA has been used to detect pathogens such as methicillin-resistant *Staphylococcus aureus* [16], *Mycobacterium tuberculosis* [17], *Acinetobacter baumannii* [18], hepatitis virus [19–21], SARS-CoV-2 [22–24], *Salmonella* [25], and porcine circovirus type 4 [26], indicating that it holds great potential as a mature detection method [27,28].

The N-terminal RNA-binding domain (NTD) and C-terminal dimerization domain (CTD) of the coronavirus nucleocapsid protein form a highly conserved functional core. The NTD binds the viral RNA packaging signal, whereas the CTD mediates N protein oligomerization. Mutations in either domain impair genome packaging or nucleocapsid assembly, making the *N* gene highly conserved and a suitable target for detection [29,30]. We therefore selected the CCoV *N* gene as the target and used the pMD20-T-N plasmid as a stable template. Based on the *N* gene sequence, three forward primers, five reverse primers, and one probe were designed. Given that increasing amplicon length reduces detection sensitivity, we systematically screened different primer combinations and selected the optimal set based on the brightest amplification bands, the shortest amplicon, and the absence of primer dimers and non-specific amplification. Reaction time and temperature were then optimized, yielding optimal conditions of 35 °C for 10 min. The analytical detection limit of the assay was 10^1 copies/μL, comparable to that of RT-qPCR. Furthermore, the conventional PCR assay targeted a much longer fragment (approximately 1461 bp), whereas the MIRA-

LFD and RT-qPCR amplicons were significantly shorter (164 bp and 128 bp, respectively). This difference in amplicon length likely contributed to the superior analytical sensitivity observed in the MIRA-LFD and RT-qPCR assays compared to conventional PCR. Notably, the assay successfully detected both the raccoon dog-associated lineage (RDCoV/CL/2022) and canine CCoV strain, while showing no cross-reactivity against nine other viral nucleic acids, demonstrating its cross-lineage detection capability.

In comparison with PCR and RT-qPCR, the MIRA-LFD assay tolerated a wide reaction temperature range of 20–45 °C, with the optimal visual readout at 35 °C. This thermal robustness is critical for on-site testing, as it reduces reliance on precisely controlled thermocyclers and allows the use of simple portable heating devices. Such flexibility lowers the risk of failed amplification under fluctuating ambient temperatures, making the assay suitable for resource-limited farms and remote veterinary clinics. However, temperatures below 20 °C or above 45 °C should be avoided, and a simple heat source remains necessary in cold environments [31].

Nucleic acid extraction is a fundamental step in molecular detection, significantly influencing both the precision and rapidity of the results. Traditional methods, such as TRIzol reagent or centrifugal column extraction kits, are cumbersome and generally take about 1 h, which greatly prolongs the overall detection time [32]. In this study, we employed the Rapid Virus RNA Extraction Kit (HaiGene Co., Ltd., Harbin, China) to extract RNA from clinical samples. This extraction process can be completed within 5 min with simple operational steps. By combining this rapid extraction with the MIRA-LFD assay, the entire detection workflow can be accomplished within 20 min, demonstrating significant potential for practical field applications.

However, there are still some limitations in this study. First, while the assay demonstrated high analytical sensitivity, the limit of detection of 10^1 copies/μL was determined using serially diluted standard recombinant plasmids. Although this provides a stable and controllable standard, it bypasses the RNA extraction and reverse transcription steps. This value should not be directly equated with the clinical limit of detection or clinical sensitivity, as complex clinical sample matrices and variations in RNA extraction efficiency may affect the actual detection capability in field samples. Second, the clinical evaluation was limited to 30 samples (22 positive and 8 negative). Although a 100% agreement was observed, the limited sample size ($n = 30$) results in wide confidence intervals (PPA:84.6–100%; NPA: 63.1–100%), restricting the precision of our estimates. This limitation stems primarily from the restricted population and sporadic disease occurrence, and future larger, multicenter studies are required to definitively confirm the clinical performance of the assay. Third, while our specificity panel included canine CCoV strain, other relevant related coronaviruses, including feline coronavirus (FCoV) and other fur-animal coronaviruses, were unavailable and thus not tested. Therefore, the current specificity claims are strictly limited to CCoV (including canine and raccoon dog hosts). Future studies are required to evaluate potential cross-reactivity with these related viruses before applying this assay to broader species populations. Fourth, despite the one-step amplification, the assay still requires tube opening for amplicon dilution and lateral flow dipstick detection, which heightens the potential risk of aerosol contamination. To mitigate this risk in field settings, physical separation of pre- and post-amplification areas (or the use of dedicated portable enclosures) and strict adherence to standard laboratory practices (e.g., using filter tips and frequent surface decontamination) are strongly recommended. Furthermore, integrating the lateral flow strip directly into a closed reaction tube represents an ideal future direction for eliminating this risk entirely [33,34]. Finally, although we obtained the complete genome sequence of one positive clinical sample (strain RDCoV/CL/2022, GenBank: OR082962) to confirm its identity, whole-genome sequencing was not performed on all positive samples due to

sample quality limitations and RNA degradation. Future studies will incorporate broader sequencing efforts to monitor potential mutations across all clinical isolates.

5. Conclusions

In this study, we developed a MIRA-LFD assay targeting the nucleocapsid gene of canine coronavirus (CCoV), including the raccoon dog-associated lineage. Compared with thermocycling-based methods such as RT-qPCR, this assay offers advantages in speed and operational simplicity, as the entire detection process (including RNA extraction, amplification, and readout) can be completed in approximately 20 min with minimal equipment. Furthermore, it demonstrated high specificity and an analytical detection limit of 10^1 copies/μL based on standard plasmid DNA. Although a preliminary evaluation of 30 clinical samples showed 100% agreement with RT-qPCR, the limited sample size and the use of plasmid standards mean that its broad diagnostic performance in routine or field conditions remains to be fully established. Future large-scale multicenter studies are warranted to confirm its clinical utility as a rapid screening tool for the target CCoV lineage.

Supplementary Materials: The following supporting information can be downloaded at: https://www.mdpi.com/article/10.3390/vetsci13121303/s1. Figure S1: Schematic illustration of the one-step RT-MIRA amplification mechanism. Reverse transcriptase first converts the viral RNA template into cDNA. The MIRA reaction utilizes a novel recombinase (helicase gp41 and recA) and single-stranded binding proteins (SSBs) to facilitate primer invasion into the double-stranded DNA. The reverse primer is 5′-biotinylated, while the probe contains a 5′-FAM label and a THF (tetrahydrofuran) residue recognized by endonuclease IV (nfo). Upon nfo cleavage, DNA polymerase extends the primers, generating double-labeled DNA amplicons (FAM and biotin) and single-stranded DNA with a FAM label. This figure was created with BioRender.com; Figure S2: Standard curve of the RT-qPCR assay. The standard curve was generated using 10-fold serial dilutions of the recombinant pMD-20T-N plasmid. The x-axis represents the logarithm of the starting quantity (Log Starting Quantity), and the y-axis represents the threshold cycle (Cq). The regression equation is $y = -3.3506x + 38.139$, with a correlation coefficient (R2) of 0.9993, and an amplification efficiency of 98.50%; Figure S3: The position of probe and primers of MIRA-LFD on the RDCoV/CL/2022 genome; Figure S4: Detection results of the 30 clinical samples. (a) Amplification curves of the RT-qPCR assay. The red curves represent the positive samples, while the green flat lines represent the negative samples. (b) Visual readout of the MIRA-LFD assay. The 30 clinical samples are numbered 1–30. Positive samples show two red lines (Control line and Test line), and negative samples show only one red line (Control line). "+" indicates the positive control, and "−" indicates the negative control. Table S1: Specimen-level details and clinical evaluation results of the 30 raccoon dog fecal samples.

Author Contributions: Conceptualization, S.Q.; methodology, S.Q.; validation, S.Q., S.C.; formal analysis, S.Q.; resources, S.Q., S.C.; data curation, S.Q.; writing—original draft preparation, S.Q.; writing—review and editing, S.Q.; visualization, S.Q.; supervision, X.X.; project administration, X.X.; funding acquisition, X.X. All authors have read and agreed to the published version of the manuscript.

Funding: This research was funded by the National Key Research and Development Program of China (Grant No. 2021YFD18011001).

Institutional Review Board Statement: Not applicable.

Informed Consent Statement: Not applicable.

Data Availability Statement: The original contributions presented in this study are included in the article/Supplementary Materials. Further inquiries can be directed to the corresponding author.

Acknowledgments: During the preparation of this manuscript, the author used ChatGPT (GPT-5.4 Professional, 2026 release; OpenAI, San Francisco, CA, USA) for the purposes of refining the abstract, introduction, discussion and conclusion of this manuscript. The authors have reviewed and edited the output and take full responsibility for the content of this publication. The schematic diagrams in Supplementary Figure S1 and the Graphical Abstract were created using BioRender.com.

Conflicts of Interest: The authors declare no conflicts of interest.

Abbreviations

The following abbreviations are used in this manuscript:

RDCoV	Raccoon Dog-associated Canine Coronavirus
CCoV	Canine Coronavirus
MIRA	Multienzyme Isothermal Rapid Amplification
LFD	Lateral Flow Dipstick
BHQ1	Black Hole Quencher 1
HPLC	high-performance liquid chromatography
RPA	recombinase polymerase amplification
RAA	Recombinase-aided amplification
NTD	N-terminal RNA-binding domain
CTD	C-terminal dimerization domain

References

1. Wang, W.; Tian, J.H.; Chen, X.; Hu, R.X.; Lin, X.D.; Pei, Y.Y.; Lv, J.X.; Zheng, J.J.; Dai, F.H.; Song, Z.G.; et al. Coronaviruses in wild animals sampled in and around Wuhan at the beginning of COVID-19 emergence. *Virus Evol.* **2022**, *8*, veac046. [CrossRef] [PubMed]
2. He, W.T.; Hou, X.; Zhao, J.; Sun, J.; He, H.; Si, W.; Wang, J.; Jiang, Z.; Yan, Z.; Xing, G.; et al. Virome characterization of game animals in China reveals a spectrum of emerging pathogens. *Cell* **2022**, *185*, 1117–1129.e1118. [CrossRef] [PubMed]
3. Cunningham-Oakes, E.; Pilgrim, J.; Darby, A.C.; Appleton, C.; Jewell, C.; Rowlingson, B.; Cuartero, C.T.; Newton, R.; Sánchez-Vizcaíno, F.; Fins, I.S.; et al. Emerging Variants of Canine Enteric Coronavirus Associated with Outbreaks of Gastroenteric Disease. *Emerg. Infect. Dis.* **2024**, *30*, 1240–1244. [CrossRef] [PubMed]
4. Ulloa, S.; Bravo, C.; Parra, B.; Ramirez, E.; Acevedo, A.; Fasce, R.; Fernandez, J. A simple method for SARS-CoV-2 detection by rRT-PCR without the use of a commercial RNA extraction kit. *J. Virol. Methods* **2020**, *285*, 113960. [CrossRef] [PubMed]
5. Ng, H.F.; Ngeow, Y.F. A simple spreadsheet-based method for relative quantification using quantitative real-time PCR. *Biochem. Mol. Biol. Educ. A Bimon. Publ. Int. Union Biochem. Mol. Biol.* **2022**, *50*, 99–103. [CrossRef] [PubMed]
6. Li, C.J.; Sun, H.Q.; Zhao, W.X.; Wang, X.Y.; Lin, R.Z.; Yao, Y.X. Rapid assay using recombinase polymerase amplification and lateral flow dipstick for identifying *Agrilus mali* (Coleoptera: Buprestidae), a serious wood-boring beetle of the western Tianshan Mountains in China. *J. Econ. Entomol.* **2023**, *116*, 1969–1981. [CrossRef] [PubMed]
7. Zhao, J.; Wan, W.; Yu, K.; Lemey, P.; Pettersson, J.H.; Bi, Y.; Lu, M.; Li, X.; Chen, Z.; Zheng, M.; et al. Farmed fur animals harbour viruses with zoonotic spillover potential. *Nature* **2024**, *634*, 228–233. [CrossRef] [PubMed]
8. Xu, L.; Cao, W.; Liu, Y.; Hu, B.; Zhang, C.; Li, S.; Liu, J.; Fu, J.; Zhang, Z.; Sun, Y.; et al. Residues 27T and 297A in VP2 contribute to the enhanced replication and pathogenicity of raccoon dog parvovirus. *J. Virol.* **2025**, *99*, e0101225. [CrossRef] [PubMed]
9. Waggoner, J.J.; Stittleburg, V.; Pond, R.; Saklawi, Y.; Sahoo, M.K.; Babiker, A.; Hussaini, L.; Kraft, C.S.; Pinsky, B.A.; Anderson, E.J.; et al. Triplex Real-Time RT-PCR for Severe Acute Respiratory Syndrome Coronavirus 2. *Emerg. Infect. Dis.* **2020**, *26*, 1633–1635. [CrossRef] [PubMed]
10. Deng, H.; Gao, Z. Bioanalytical applications of isothermal nucleic acid amplification techniques. *Anal. Chim. Acta* **2015**, *853*, 30–45. [CrossRef] [PubMed]
11. Lobato, I.M.; O'Sullivan, C.K. Recombinase polymerase amplification: Basics, applications and recent advances. *Trends Anal. Chem. TRAC* **2018**, *98*, 19–35. [CrossRef] [PubMed]
12. Zhang, X.; Guo, L.; Ma, R.; Cong, L.; Wu, Z.; Wei, Y.; Xue, S.; Zheng, W.; Tang, S. Rapid detection of *Salmonella* with Recombinase Aided Amplification. *J. Microbiol. Methods* **2017**, *139*, 202–204. [CrossRef] [PubMed]
13. Rohrman, B.A.; Richards-Kortum, R.R. A paper and plastic device for performing recombinase polymerase amplification of HIV DNA. *Lab A Chip* **2012**, *12*, 3082–3088. [CrossRef] [PubMed]
14. Park, S.B.; Zhang, Y. Development of Multienzyme Isothermal Rapid Amplification (MIRA) Combined with Lateral-Flow Dipstick (LFD) Assay to Detect Species-Specific tlh and Pathogenic trh and tdh Genes of *Vibrio parahaemolyticus*. *Pathogens* **2024**, *13*, 57. [CrossRef] [PubMed]
15. Tan, M.; Liao, C.; Liang, L.; Yi, X.; Zhou, Z.; Wei, G. Recent advances in recombinase polymerase amplification: Principle, advantages, disadvantages and applications. *Front. Cell. Infect. Microbiol.* **2022**, *12*, 1019071. [CrossRef] [PubMed]
16. Ding, X.; Wang, H.; Cui, M.; Cheng, M.; Zhao, Q.; Bai, Y.; Zhang, C.; Zhang, C.; Xu, S.; Li, T. Development of a Real-Time Recombinase-Aided Amplification Method to Rapidly Detect Methicillin-Resistant *Staphylococcus aureus*. *Microorganisms* **2022**, *10*, 2351. [CrossRef] [PubMed]

17. Liu, Y.; Ren, W.; Xue, Z.; Miao, Y.; Wang, W.; Zhang, X.; Yao, C.; Shang, Y.; Li, S.; Mi, F.; et al. Real-time recombinase-aided amplification assay for rapid amplification of the IS1081 gene of *Mycobacterium tuberculosis*. *Eur. J. Clin. Microbiol. Infect. Dis. Off. Publ. Eur. Soc. Clin. Microbiol.* **2023**, *42*, 963–972. [CrossRef] [PubMed]
18. Hu, W.W.; He, J.W.; Guo, S.L.; Li, J. Development and evaluation of a rapid and sensitive multienzyme isothermal rapid amplification with a lateral flow dipstick assay for detection of *Acinetobacter baumannii* in spiked blood specimens. *Front. Cell. Infect. Microbiol.* **2022**, *12*, 1010201. [CrossRef] [PubMed]
19. Sun, M.L.; Zhong, Y.; Li, X.N.; Yao, J.; Pan, Y.Q. Simple and feasible detection of hepatitis a virus using reverse transcription multienzyme isothermal rapid amplification and lateral flow dipsticks without standard PCR laboratory. *Artif. Cells Nanomed. Biotechnol.* **2023**, *51*, 233–240. [CrossRef] [PubMed]
20. Zhu, C.; Li, J.; Yu, H.; Xu, K.; He, X.; Liu, Z.; Chen, J. CRISPR/Cas13a combined with reverse transcription-multienzyme isothermal rapid amplification for hepatitis B virus RNA detection. *Anal. Chim. Acta* **2025**, *1370*, 344389. [CrossRef] [PubMed]
21. Sun, M.L.; Lai, H.Y.; Chong, N.Y.; Liu, D.F.; Zhang, Z.Y.; Pang, B.; Yao, J. Simple and Feasible Detection of Hepatitis B Virus via Combination of Multienzyme Isothermal Rapid Amplification and Lateral Flow Dipstick Strip. *Front. Mol. Biosci.* **2021**, *8*, 763079. [CrossRef] [PubMed]
22. Liu, H.; Chang, S.; Chen, S.; Du, Y.; Wang, H.; Wang, C.; Xiang, Y.; Wang, Q.; Li, Z.; Wang, S.; et al. Highly sensitive and rapid detection of SARS-CoV-2 via a portable CRISPR-Cas13a-based lateral flow assay. *J. Med. Virol.* **2022**, *94*, 5858–5866. [CrossRef] [PubMed]
23. Meng, X.; Zou, S.; Li, D.; He, J.; Fang, L.; Wang, H.; Yan, X.; Duan, D.; Gao, L. Nanozyme-strip for rapid and ultrasensitive nucleic acid detection of SARS-CoV-2. *Biosens. Bioelectron.* **2022**, *217*, 114739. [CrossRef] [PubMed]
24. Shang, M.; Li, J.; Sun, X.; Su, N.; Li, B.; Jiang, Y.; Chong, H.; Lu, W.; Huang, Q. Duplex Reverse Transcription Multienzyme Isothermal Rapid Amplification Assays for Detecting SARS-CoV-2. *Clin. Lab.* **2021**, *67*, 2517. [CrossRef] [PubMed]
25. Wu, S.; Duan, H.; Zhang, Y.; Wang, S.; Zheng, L.; Cai, G.; Lin, J.; Yue, X. A Salmonella Microfluidic Chip Combining Non-Contact Eddy Heater and 3D Fan-Shaped Mixer with Recombinase Aided Amplification. *Biosensors* **2022**, *12*, 726. [CrossRef] [PubMed]
26. Li, Y.; Zhao, Y.; Li, C.; Yang, K.; Li, Z.; Shang, W.; Song, X.; Shao, Y.; Qi, K.; Tu, J. Rapid detection of porcine circovirus type 4 via multienzyme isothermal rapid amplification. *Front. Vet. Sci.* **2022**, *9*, 949172. [CrossRef] [PubMed]
27. Zeng, F.; Wu, M.; Ma, L.; Han, Z.; Shi, Y.; Zhang, Y.; Liu, C.; Zhang, S.; Cong, F.; Liu, S. Rapid and sensitive real-time recombinase polymerase amplification for detection of Marek's disease virus. *Mol. Cell. Probes* **2019**, *48*, 101468. [CrossRef] [PubMed]
28. Fan, Y.; Wang, J.; Bian, X.; Wang, W.; Zhou, J.; Zhang, X.; Hu, M.; Sun, M.; Yang, S.; Zhao, Y.; et al. Multienzyme isothermal rapid amplification (MIRA)-LFD assay for rapid detection of PEDV and PoRVA. *J. Microbiol. Methods* **2025**, *238*, 107289. [CrossRef] [PubMed]
29. Farsang, A.; Ros, C.; Renström, L.H.; Baule, C.; Soós, T.; Belák, S. Molecular epizootiology of infectious bronchitis virus in Sweden indicating the involvement of a vaccine strain. *Avian Pathol.* **2002**, *31*, 229–236. [CrossRef] [PubMed]
30. Patil, S.M.; Srinivasa, C.; Ramu, R.; Kollur, S.P.; Ramesh, S.; Shivamallu, C. Chapter 1—SARS-CoV-2 genome sequencing and promising druggable targets. In *Coronavirus Drug Discovery*; Egbuna, C., Ed.; Elsevier: Amsterdam, The Netherlands, 2022; pp. 3–22.
31. Lorenz, T.C. Polymerase chain reaction: Basic protocol plus troubleshooting and optimization strategies. *J. Vis. Exp. JoVE* **2012**, *63*, e3998. [CrossRef] [PubMed]
32. Ali, N.; Rampazzo, R.C.P.; Costa, A.D.T.; Krieger, M.A. Current Nucleic Acid Extraction Methods and Their Implications to Point-of-Care Diagnostics. *BioMed Res. Int.* **2017**, *2017*, 9306564. [CrossRef] [PubMed]
33. El-Tholoth, M.; Bau, H.H. Molecular Detection of Respiratory Tract Viruses in Chickens at the Point of Need by Loop-Mediated Isothermal Amplification (LAMP). *Viruses* **2024**, *16*, 1248. [CrossRef] [PubMed]
34. Daher, R.K.; Stewart, G.; Boissinot, M.; Bergeron, M.G. Recombinase Polymerase Amplification for Diagnostic Applications. *Clin. Chem.* **2016**, *62*, 947–958. [CrossRef] [PubMed]

Disclaimer/Publisher's Note: The statements, opinions and data contained in all publications are solely those of the individual author(s) and contributor(s) and not of MDPI and/or the editor(s). MDPI and/or the editor(s) disclaim responsibility for any injury to people or property resulting from any ideas, methods, instructions or products referred to in the content.